Characterization and functionalization of nanostructured indium tin oxide films

Author: Marta Viñas Calaf
Facultat de Física, Universitat de Barcelona, Diagonal 645, 08028 Barcelona, Spain.

Advisor: Manel López de Miguel

Abstract: We revise the ability of developing electrochemical biosensors made of indium tin oxide (ITO) through the fabrication, characterization and functionalization of nanostructured ITO electrodes. Self-made nanostructured ITO thin film and nanostructured electrodes were obtained by electron beam evaporation and the difference in morphology was confirmed by scanning electron microscopy (SEM). A high conductivity value ($\sim 10^6$ mS/cm) for self-fabricated and commercial samples was confirmed by the four points probe method. Cyclic voltammetry (CV) confirmed an increase in the electroactive surface area of ITO nanowires with respect to thin ITO films and commercial samples, implying possible higher detection levels. To study the detectability of nanostructured ITO surfaces, chemical functionalization was carried out. Fourier transform infrared spectroscopy (FTIR) confirmed that functionalization was correctly done and electrochemical impedance spectroscopy (EIS) showed that functionalized electrodes present higher polarization resistance, acting as an electronic barrier for the electron transfer between the ionic solution and the ITO electrode. These results are a first step to prove the benefits of sensing by using electrochemical biosensors, based on nanostructured ITO electrodes.

I. INTRODUCTION

Nowadays, quantification of biological or biochemical processes is extremely important in fields such as Biotechnology, Biology or Medicine. However, converting the biological information to an easily processed electronic signal is challenging due to the complexity of connecting an electronic device directly to a biological environment. Biosensors, in particular electrochemical ones, are analytical devices which provide an attractive way to analyze the content of biological samples due to the direct conversion of a chemical event to an electronic signal. The biosensor has two distinguishable parts: the recognition part, where a biological event takes place (either as a chemical or physical reaction), and the transducer part, where the energy of the reaction is transformed into something measurable, typically electrical current.

Lately, biosensors are becoming increasingly important in the biomedical field and a wide variety of them are being used as diagnostic tools. However, there is a lack of sensitive, fast, cost-effective and miniaturized biological detection sensors [1]. Transparent Conductive Oxides (TCOs) may be a suitable material to develop high quality biosensors, as they have proven to be integrable with the silicon chip technology or in other fields such as optoelectronic devices. Examples of TCOs are tin, indium, zinc and cadmium oxides, as well as their various alloys. In particular, there has been a growing interest in the fabrication of biosensors employing indium tin oxide (ITO) due to its optimal electrical and optical behaviour. ITO is a n-type highly degenerated semiconductor and possesses a wide energy band gap around 3.6 eV. Moreover, it possess a good electrical conductivity, high optical transmission in the visible wavelength region, high reflectance in the near- infrared (IR) region [2, 3].

For the purpose of developing ultrasensitive electrochemical biosensors, nanomaterials have been a key starting point due to their favourable electronic properties, electrocatalytic activity and high surface-to-volume ratio, which makes their electrical properties increasingly susceptible to external influences [1]. The covalent attachment process of specific biomolecules to conductive surfaces is of great importance for an optimal molecular recognition. An intermediate layer of molecules which promote the binding of organic molecules into the inorganic substrate is needed. These are known as silane compounds and have been used for many years as adhesive agents to promote the aforementioned binding [4]. In the present work, 3-glycidoxypropyltrimethoxylane (GOPTS) is the intermediate molecule chosen to functionalize ITO substrates as it has been reported to be very useful for biosensing purposes [4–6].

This work consists in a study of the viability of nanostructured films as a material for biosensing applications through characterization and chemical functionalization by attaching organic molecules onto them. Commercial (cITO) and self-developed samples, nanostructured (nITO) and thin ITO film (tfITO), have been used in this study. The present document is structured in different sections. The section II includes a detailed explanation on materials, parameters and techniques used to develop the study such as electron beam evaporation (EBE) to fabricate the electrodes, various methods like scanning electron microscopy (SEM), energy-dispersive X-ray spectroscopy (EDS), electrochemical impedance spectroscopy (EIS) or cyclic voltammetry (CV) to characterize the samples. Also a detailed immunoassay used to functionalize the samples is explained. Afterwards, the characterization and further results are discussed in the section III, and a conclusion is presented in IV.

II. MATERIAL AND METHODS

A. Electrodes fabrication

Thin ITO films and nITO were deposited on glass substrates using EBE (Pfeiffer vacuum classic 500). Glass slides were previously cleaned in acetone and ethanol for 10 minutes, rinsed with deionized (DI) water (MilliQ, Millipore) and finally dried in a stream of nitrogen. The target material used in this study was pellet-shaped ITO with a composition of 90 % In_2O_3 - 10 % SnO_2 (Neyco, France). Commercial ITO samples, which have also been under study, were purchased from Sigma Aldrich, Spain.

The electron beam machine was programmed to generate the ITO samples at a rate of 1 Å/s with a final thickness of 500 nm at a temperature of 500 °C for nITO electrodes and 100 °C for tfITO electrodes. The deposited samples were annealed in a furnace for 1 hour at 700 °C to promote the ITO crystallisation and the enhancement of electrical conductivity.

B. Substrate characterization

Thin ITO films and cITO samples were characterized studying their resistivity by a four points probe station (Keysight B2912A Precision Source/Measure Unit). The compositional studies of the samples were determined by EDS which worked under the SEM, also used for observing the surface morphology. Basic electrochemical methods such as EIS and CV, were carried out in a conventional three-electrode electrochemical cell, with a 5 mM solution of the redox pair ferrocyanide/ferricyanide ($K_4Fe(CN)_6/K_3Fe(CN)_6$) in a 100 mM KCl electrolyte solution. A platinum wire was used as a counter electrode, Ag/AgCl in saturated KCl was used as a commercial reference electrode, and the working electrode was the ITO sample under study. The electrode geometrical projected area exposed to the redox solution was defined by the inner diameter of a O-ring of 0.7 cm^2. A Biologic-EC-Lab SP3150 potentiostat analyzer was used to conduct the electrochemical experiments.

C. Substrate functionalization

ITO surfaces were first cleaned and prepared for derivatization. All slides were immersed in ethanol, acetone and DI water for 5 minutes and then, dried with a stream of nitrogen. After, the samples were treated with UV-Ozone for 20 minutes. For ITO silanization, a solution of GOPTS at 2.5 % (v/v) in anhydrous ethanol (100 %) was prepared. All slides were immersed in the prepared solution and left in the oven for 30 minutes at 37 °C. Then, they were rinsed in ethanol and dried with a stream of nitrogen.

The next step was the functionalization with the bovine serum albumin (BSA) antibody. A drop of 50 μl with a concentration of 50 mg/ml of BSA in phosphate buffer saline (PBS) was deposited on each sample. Isolated from light, the reaction was let take place for 30 minutes and afterwards the samples were cleaned with PBS, DI water and dried with a stream of nitrogen.

At this point, anti-BSA (antigen) immobilization was carried out. The experiments were done at two different concentrations: 1/3 of the samples were covered using a 1/1000 anti-BSA concentration, another 1/3 were covered using a 1/3000 anti-BSA concentration whereas the remaining 1/3 were not covered with anti-BSA, but with pure phosphate buffer saline tween (PBST) as blank samples. The reaction was let take place for 30 minutes and then the samples were cleaned with PBST. The last step consisted in the immobilization of the enzyme anti-IgG-HRP at a constant concentration of 1/1000 in PBST.

Once the substrate functionalization was done, additional measurement techniques like FTIR were carried out as a helpful indirect method to confirm the presence of attached biomolecules on the ITO surfaces. Moreover, EIS was performed for a semi quantitative analysis and the results were fitted as a model biosensor, specifically as an equivalent electronic circuit [10].

III. RESULTS AND DISCUSSION

Substrate characterization

The conductivity of the samples was tested by the four point probe method. The value obtained for tfITO electrodes (8.21×10^5 mS/cm) was slightly lower in comparison with the commercial sample (3.82×10^6 mS/cm) due to the difference in tin and indium concentrations seen by EDS. The conductivity of nITO electrodes cannot be obtained through this method due to the lack of knowledge about nanowires dimensions and their placement onto the glass surface. However, the tin/indium ratios appear to be similar to tfITO samples. Possible changes may be done in future works in order to achieve a higher conductivity value, such as adjustments of annealing temperature or dopant concentrations, which have been reported to contribute to the enhancement of conductivity values [3, 7].

Additionally, surface morphology of both kinds of ITO electrodes was analyzed by SEM. Thin ITO film is in-

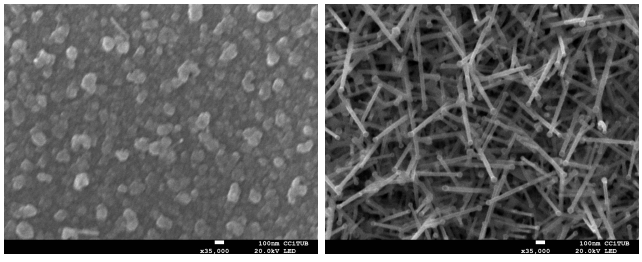

(a) tfITO (b) nITO

FIG. 1: SEM images of ITO-deposited electrodes ×35,000.

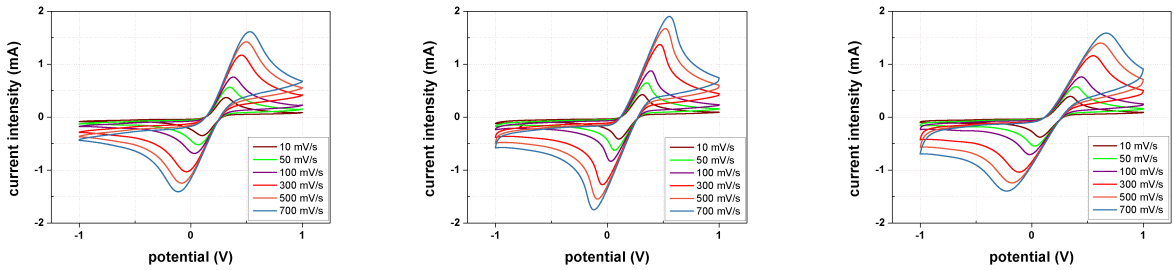

(a) cITO (b) nITO (c) tfITO

FIG. 2: Representation of intensity vs. electrode potential (cyclic voltammetry) at different scan rates (10 mV/s, 50 mV/s, 100 mV/s, 300 mV/s, 500 mV/s and 700 mV/s) for the three types of electrodes. Three repetitive cycles were applied from -0.9 V to 0.9 V for each scan rate.

	cITO			nITO			tfITO		
υ [V/s]	$E_{1/2}[V]$	ΔE_p [V]	i_{pa}/i_{pc} [V]	$E_{1/2}[V]$	ΔE_p [V]	i_{pa}/i_{pc} [V]	$E_{1/2}[V]$	ΔE_p [V]	i_{pa}/i_{pc} [V]
0.02	0.21	0.21	1.09	0.21	0.20	1.00	0.21	0.28	1.04
0.05	0.21	0.27	0.92	0.21	0.27	1.06	0.21	0.38	0.97
0.10	0.21	0.34	1.14	0.21	0.34	0.98	0.24	0.43	1.04
0.30	0.24	0.42	1.16	0.25	0.42	1.04	0.34	0.44	0.97
0.50	0.28	0.42	1.28	0.29	0.43	1.12	0.41	0.44	1.09
0.70	0.32	0.42	1.44	0.32	0.43	0.99	0.46	0.45	1.26

TABLE I: Summary of values for the quasi-reversible parameters.

tegrated by a lot of small grains which can be observed in Fig. 1(a) whereas in Fig. 1(b) nITO formation can be clearly appreciated being randomly forest-like distributed. The morphological difference between both depositions is related to the increase of functional surface to volume ratio, which has already been reported in [8]. An increase in geometrical surface area for nITO electrodes in comparison with tfITO has been reported [4]. The electroactive area was deduced by the CV parameters analysis through the cathodic and anodic currents and the potentials at which the species on the sensor surface were reduced or oxidized.

The CV profiles shown in Fig. 2 reveal a quasi-reversible heterogeneous charge transfer process. The peak potential separation defined as the difference between the oxidation and reduction peak potentials ($\Delta E_p = E_{pa}$ - E_{pc}) increases when increasing the scan rate (υ), the current ratio of the oxidation and reduction current peak (i_{pa}/i_{pc}) is around the unity at all scan rates and the current peak shifts in potential with scan rate so the potential at which the half current $E_{1/2}$ is observed increase when increasing the scan rate [8, 9]. Table 1 shows the values obtained for the mentioned parameters. There is a similar reversibility between cITO and nITO electrodes which is due to the similar values of ΔE_p. Moreover, nITO electrodes present the shortest peak-to-peak separation in each voltammogram, which is related to the speed of the electrons involved in the following redox reaction due to the interaction between the electrode and the ferricyanide/ferrocyanide solution.

$$[Fe(CN)_6]^{4-} \longleftrightarrow [Fe(CN)_6]^{3-} + e^-$$

In the case of quasi-reversibility, the rate of electron transfer becomes comparable to the mass transport rate. Taking into account the interaction between the electrode and the solution, it can be assumed that diffusion is the most significant mass transport process in the movement of material above migration and convection contributions, which can be neglected [8, 9].

When the electrolysis reactions take place, the reactants close to the electrode surface are consumed and consequently a concentration gradient appears. To support further electrolysis, an amount of fresh reactant from the bulk solution reaches the solution-electrode interface. The rate of diffusion is controlled by the concentration gradient.

The electrode area calculation was done using the following Randles-Sevcik equation for a quasi-reversible system:

$$I_{peak}^{quasi} = (2.65 \times 10^5) n^{3/2} AC(D\upsilon)^{1/2} \quad (1)$$

Where I_{peak}^{quasi} is the maximum current of oxidation in amperes, n is the total number of electrons transferred for each molecule in the redox process (one in the present case), A is the geometric area of the electrode in cm^2, D is the diffusion constant in cm^2/s, C is the concentration of the solution in mol/cm^3 and υ is the scan rate in V/s.

The magnitude of the voltammetric current observed at the electrode is proportional to the applied voltammetric scan rate. Thus, the oxidation current intensity peak (I_{peak}^{quasi}) against square root of scan rates ($\upsilon^{1/2}$) was plotted, and a linear fitting was performed in order to obtain the slope value, from which the electroactive area

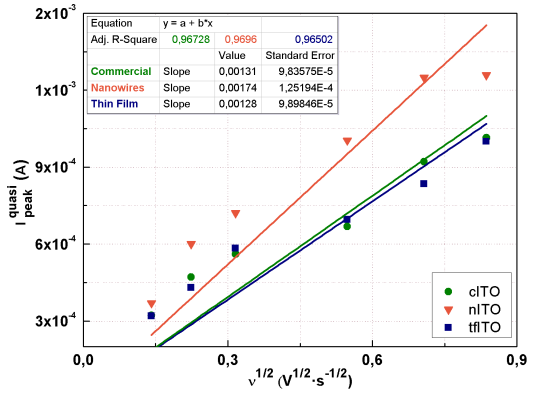

FIG. 3: Representation of intensity peak in amperes against square root of scan rate in mV/s. A linear equation was adjusted for each dataset and the electroactive surface area was calculated for each type of electrode by the slope.

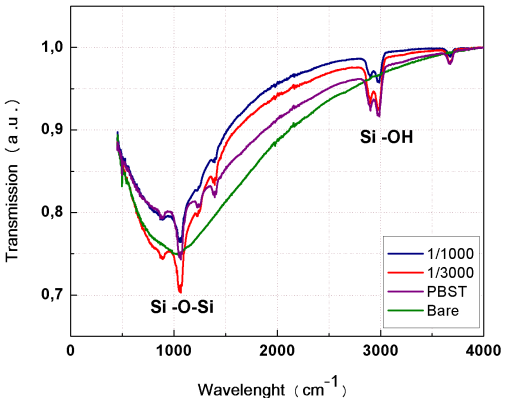

FIG. 4: FTIR spectra of bare and GOPTS-functionalized ITO electrodes, recorded in the wavelength region 500 - 4000 cm^{-1}.

was calculated. The linear representation of equation (1) and the fitting parameters are shown in Fig. 3.

An electroactive area of 0.36 cm^2, 0.25 cm^2, 0.26 cm^2, was deduced for nITO, tfITO and cITO respectively. This means that nITO have more surface available for exchanging electrons with the interface, which means higher current. The corroboration of these results implies that nITO electrodes should increase biosensor sensitivity due to their high value of conductivity and larger electroctive surface area compared to tfITO elctrodes. To prove this, biofunctionalization of nITO and cITO samples, which worked intrinsically better than tfITO, was performed and the results are discussed below.

Substrate functionalization

As a first step to test the functionalization of the set of samples, the transmittance infrared spectra was carried out and is shown in Fig. 4. Differences between bare ITO and organosilane-functionalized ITO substrates were quite significant. The peaks obtained for functionalized electrodes indicated a drop in transmittance due to the presence of attached molecules onto the surfaces whilst no peaks appeared for the bare sample. These peaks can be assigned to the covalent bond formation as a result of GOPTS functionalization. The drop in wavelenght value of 1060 cm^{-1} can be attributed to Si-O-Si bond formation and the peaks in 2900 cm^{-1} and 3000 cm^{-1} can be assigned to the Si-OH bonds [9].

Semi-quantitative EIS analysis of the functionalization process was done to the functionalized samples by fitting the data to an equivalent circuit model known as Randles circuit [10]. It includes a solution resistance (R_s), a double layer capacitance (C_{dl}) in parallel with the polarization resistance (R_p) and the Warburg impedance (Z_W). The Nyquist Diagram for cITO and the equivalent circuit is shown in Fig. 5. The solution resistance can be found by reading the real axis value at the high frequency intercept. The low-frequency zone intercepts the sum of the polarization resistance and the solution resistance. The Warburg impedance, used to simulate the mass-transport effects, appears as a straight line of 45°.

GOPTS-functionalized surfaces present both higher polarization resistance and double-layer capacitance values in the low-frequency range respect to the bare substrates. Fig. 6(a) and Fig. 6(b) show the EIS measurements on bare and functionalized ITO electrodes. This means that the attached organic layer acts as an isolator between the ITO electrodes and its surrounding electrolyte impeding the electron transference. Moreover, these parameters increase when increasing the anti-BSA concentration obtaining the highest value for 1/1000 concentration. On nITO samples, the diffusion term, appearing as a straight line on the representations, is more significant than the double layer capacitance due to nanowires branched morphology, which prevents the ions in solution to form a double layer capacitor on the electrode surface. Despite the differences obtained, the Nyquist diagram for nITO and cITO follows the same tendency.

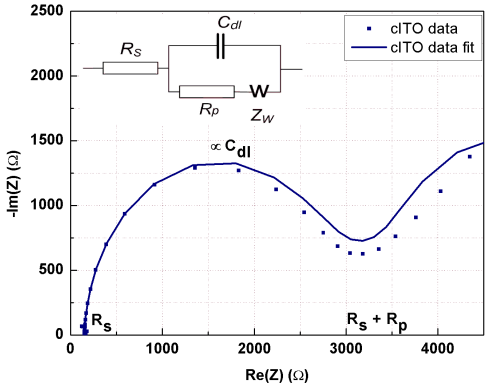

FIG. 5: Nyquist Diagram for cITO and the respective adjustment to the Randles Equivalent Circuit inserted above.

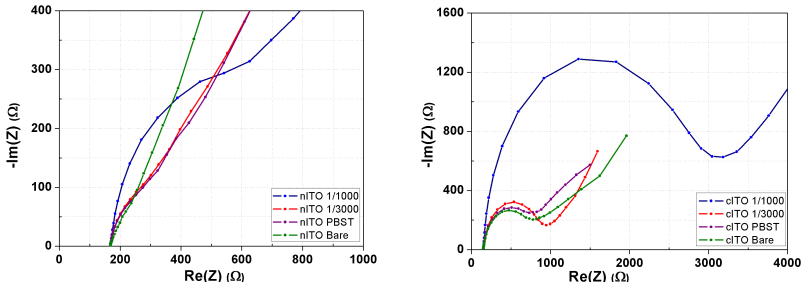

(a) nITO (b) cITO

FIG. 6: EIS results for functionalized samples.

IV. CONCLUSIONS

The semi-quantitative results of EIS obtained for nITO samples are not clear enough to be easily interpreted, due to the complexity of the nanostructured morphology. The double layer between the electrode and the electrolyte is weakly formed for branched ITO samples and it is not possible to determine the parameters of the equivalent Randles circuit model. Therefore, a quantitative comparison of the detectability between nITO and cITO samples cannot be performed. However, higher sensitivity for nITO in comparison with tfITO and cITO samples has been deduced after CV analysis. Nanostructured ITO films present higher electroactive area than tfITO and cITO samples, permitting an increase of intensity current when redox reactions take place.

Also, it has been proven that nITO samples can be functionalized by fixing organic molecules onto the electrodes. The electron transfer between redox species in solution and conducting ITO substrates is affected by the organic layer attached, which behaves as an electronic barrier and increases the polarization resistance and the double-layer capacitance values.

Additionally, this work proves that a first step can be done for developing sensitivity-enhanced bioelectronics that may be fully integrated in a future with the silicon chip technology. The obtained results may indicate that a basic functionalization of nITO electrodes is possible and future works will be focused on the improvement of the quantification methods to study the sensitivity of the sensors.

Acknowledgments

I would like to express my sincere gratitude to Raquel Pruna for her patient guidance, valuable help and willingness to give her time so generously. I would also like to thank my advisor Manel López for all his helpful comments and corrections and Mónica Martínez for her eagerness to help. Thanks to Dr. Blas Garrido and his team for lending us the nanotechnology platform facilities, specially the electron beam machine. Thanks also to my family and friends for the support throughout this years.

[1] D.Grieshaber, R.MacKenzie, J.Vörös and E.Reimhult. 2008 Electrochemical Biosensors Sensor Principles and Architectures. *Sensors* **8**, 1400-1458.

[2] R.Rakesh Kumar, K.Narashimha Rao, K.Rajanna, A.R Phani. 2014 Low temperature and self catalytic growth of ultrafine ITO nanowires by electron beam evaporation method and their optical and electrical properties. *Material Research Bulletin* **52**, 167176.

[3] J.George, C.S. Menon. 2000 Electrical and optical properties of electron beam evaporated ITO thin films. *Surface and Coatings Technology* **132**, 45-48.

[4] R.Pruna, F.Palacio, M.Martínez, O.Blázquez, S.Hernández, B.Garrido, M.López. 2016 Organosilane-functionalization of nanostructured indium tin oxide films. *Interface Focus*.

[5] L.Yang, Y.Li. 2005 AFM and impedance spectroscopy characterization of the immobilization antibodies on indium-tin oxide electrode through self-assembled monolayer of epoxysilane and their capture of Escherichia coli 0157:H7. *Biosens. Bioelectron.* **20**, 1407-1416.

[6] H.Hillebrandt, M.Tanaka. 2001 Electrochemical characterization of self-assembled alkylsiloxane monolayers on indium-tin oxide (ITO) semiconductor electrodes.*J. Phys. Chem. B* **105**, 4270-4276.

[7] M.Yamaguchi, A.Ide-Ektessabi, H.Nomura, N.Yasui. 2004 Characteristics of indium tin oxide thin films prepard using electron beam evaporation. *Thin Solid Films* 447-448.

[8] R.Pruna, F.Palacio, M.López, J.Pérez, M.Mir, O.Blázquez, S.Hernández, B.Garrido. 2016 Electrochemical characterization of organosilane-functionalized nanostructured ITO surfaces. *Applied Physics Letters* **109**:6.

[9] E.Pretsch, P.Bühlmann, C.Affolter. Structure Determination of Organic Compounds. Tables of Spectral Data.

[10] J.P. Diard, B.Le Gorrec, C. Montella. 2012 Handbook of Electrochemical Impedance Spectroscopy.